

Updated Constraints on Self-Interacting Dark Matter from Supernova 1987A

Cameron Mahoney,^{1,*} Adam K. Leibovich,^{1,†} and Andrew R. Zentner^{1,‡}

¹*Pittsburgh Particle Physics Astrophysics and Cosmology Center (PITT PACC)*

Department of Physics and Astronomy, University of Pittsburgh, Pittsburgh, Pennsylvania 15260, USA

We revisit SN1987A constraints on light, hidden sector gauge bosons (“dark photons”) that are coupled to the standard model through kinetic mixing with the photon. These constraints are realized because excessive bremsstrahlung radiation of the dark photon can lead to rapid cooling of the SN1987A progenitor core, in contradiction to the observed neutrinos from that event. The models we consider are of interest as phenomenological models of strongly self-interacting dark matter. We clarify several possible ambiguities in the literature and identify errors in prior analyses. We find constraints on the dark photon mixing parameter that are in rough agreement with the early estimates of Dent et al. [52], but only because significant errors in their analyses fortuitously canceled. Our constraints are in good agreement with subsequent analyses by Rrapaj & Reddy [53] and Hardy & Lasenby [54]. We estimate the dark photon bremsstrahlung rate using one-pion exchange (OPE), while Rrapaj & Reddy use a soft radiation approximation (SRA) to exploit measured nuclear scattering cross sections. We find that the differences between mixing parameter constraints obtained through the OPE approximation or the SRA approximation are roughly a factor of $\sim 2 - 3$. Hardy & Lasenby [54] include plasma effects in their calculations finding significantly weaker constraints on dark photon mixing for dark photon masses below ~ 10 MeV. We do not consider plasma effects. Lastly, we point out that the properties of the SN1987A progenitor core remain somewhat uncertain and that this uncertainty alone causes uncertainty of at least a factor of $\sim 2 - 3$ in the excluded values of the dark photon mixing parameter. Further refinement of these estimates is unwarranted until either the interior of the SN1987A progenitor is more well understood or additional, large, and heretofore neglected effects, such as the plasma interactions studied by Hardy & Lasenby [54], are identified.

I. INTRODUCTION

An overwhelming preponderance of observational evidence indicates that a form of nonrelativistic, nonbaryonic, dark matter constitutes the majority of mass in the Universe and drives the formation of cosmic structure. The pace of the quest to identify the dark matter is accelerating on many fronts. Weakly-interacting massive particles (WIMPs) have received the most attention as dark matter candidates (see Ref. [1] for a review). Dark matter particles that interact with standard model particles only weakly, while interacting among themselves much more strongly have been studied as an alternative to WIMP scenarios in numerous contexts [2–20] and constraints on self-interacting dark matter (SIDM) models have been explored by many authors [21–49]. In this paper, we revisit and update astrophysical constraints on SIDM models from supernova cooling.

SIDM models in which large self-interaction cross sections are mediated by sufficiently light bosons ($M \lesssim 100$ GeV) can be constrained astrophysically using supernovae, particularly SN1987A. Light gauge bosons will be produced within the hot supernova core, primarily through bremsstrahlung, and radiated. This non-standard energy loss mechanism can result in an energy loss rate from the supernova core that is inconsistent with observations of neutrinos from SN1987A, analogous to the classic constraint on axions [50, 51]. This effect has already been exploited by Dent et al. [52], Rrapaj and Reddy [53], and Hardy and Lasenby [54] to constraint dark electromagnetism models in which the new gauge boson, the so-called dark photon, is kinetically mixed with the standard model photon. See also [55–57]. The SN1987A constraint places a limit on the mixing parameter.

We initiated our study because of a number of ambiguities appearing in the previous literature on this subject. In particular, we could not reproduce the constraints of Ref. [52]. During the course of our study, we identified a number of errors in the analysis of Ref. [52]. First, it is straightforward to demonstrate that the kinematical relationships given in Appendix A of Ref. [52] are incorrect.

*E-mail:cbm34@pitt.edu

†E-mail:akl2@pitt.edu

‡E-mail:zentner@pitt.edu

Second, the squared matrix elements given in Eq. (A3) and Eq. (C18) of Ref. [52] must be incorrect. These matrix elements do not obey the correct symmetries under interchange of incoming and/or outgoing momenta. Furthermore, Ref. [52] neglects the mass of the gauge boson, which is legitimate in the classic case of the \sim meV-mass axion, but not in the present context. Finally, Ref. [52] employed an inconsistent model for the permitted energy loss rate from the supernova interior. Our work amounts primarily to repeating the calculation of Ref. [52] in order to rectify these oversights. Our primary calculation treats nucleon scattering via one-pion exchange (OPE).

As we were completing our manuscript, two related papers were published. Rrapaj and Reddy [53] computed bounds on mixing of the dark and standard model photons using a soft radiation approximation (SRA) for dark photon bremsstrahlung. This has the distinct advantage of enabling nucleon scattering data to be used directly in the estimation of the bremsstrahlung rate, but is only approximate because at large dark photon masses the radiated dark photons carry off considerable momentum and energy. We have been able to reproduce the result of Rrapaj and Reddy [53] and find that the SRA plausibly results in only a factor of ~ 3 underestimate of the upper bound on the dark photon mixing parameter at most. Moreover, our OPE results agree well with the SRA calculation of Rrapaj and Reddy [53]. Nonetheless, Ref. [53] quote results very similar to those of Dent et al. [52]. We find, rather remarkably, that the various errors in the analysis of Ref. [52] conspire to yield a constraint that is very similar to the correct answer.

More recently, Hardy and Lasenby [54] studied bounds on these same models (and others) including plasma effects. For simplicity, we have not included these plasma effects in our calculations. Hardy and Lasenby base their calculation off of the SRA of Ref. [53]. Consequently, for dark photon masses $\gtrsim 10$ MeV they find very similar results to Ref. [53] as well as the constraints we present in this manuscript. For dark photon masses $\lesssim 10$ MeV, Hardy and Lasenby demonstrate that constraints on the dark photon mixing parameter are significantly weaker than one finds when neglecting plasma effects [54].

It is important to delineate correctly the range of the viable parameter space for SIDM models. The parameter space available to dark electromagnetism models of SIDM has been studied extensively not only in the aforementioned papers, but also in the work of Bjorken et al. [58] and the Snowmass white paper by Kaplinghat, Tulin, and Yu [59]. One point that is clear from previous work is that there is at most only a slim sliver of parameter space that can simultaneously yield the correct relic abundance of SIDM through thermal production, have

interesting effects on cosmological structure formation, and evade all constraints including the constraints from SN1987A. In accord with Ref. [53] and Ref. [54], we find that the constraints quoted in Ref. [52] are too restrictive, but only by a factor of ~ 4 due to a conspiratorial cancellation of errors in Ref. [52]. Hardy and Lasenby go on to demonstrate that these constraints are significantly too restrictive for dark photon masses $\lesssim 10$ MeV due to plasma effects.

The remainder of this paper is organized as follows. In Section II, we discuss dark photon models. We describe our calculation of SN1987A constraints on SIDM in Section III and present our primary results in Section IV. We stress only those points that are key to understanding the relationship between our work and the work of both Dent et al. in Ref. [52] and Rrapaj and Reddy in Ref. [53]. We summarize our work and draw conclusions in Section V.

II. DARK PHOTON MODEL OF SIDM

We consider constraints on SIDM specifically within the context of dark electromagnetism models. Dark electromagnetism models are models in which a hidden, dark sector contains a broken $U(1)'$ symmetry and the $U(1)'$ gauge boson is kinetically mixed with the standard model photon. For the purposes of this study, this is important because it demands that the Lagrangian contains terms such as

$$\mathcal{L}_{\text{int}} = g_{\chi} \bar{\chi} \tilde{A}' \chi + q \bar{f} \tilde{A} f, \quad (1)$$

where χ is the dark matter, g_{χ} is the dark coupling, \tilde{A}' is the dark gauge boson, f is a standard model fermion of charge q , and \tilde{A} is the standard model gauge boson. The kinetic mixing, through a term $\frac{1}{2} \frac{\epsilon}{\sqrt{1+\epsilon^2}} \tilde{F}_{\mu\nu} \tilde{F}'^{\mu\nu}$ in the Lagrangian causes the \tilde{A} to be an admixture of the massless photon A , and the dark photon A' , of mass $m_{A'} = m_{\tilde{A}'} \sqrt{1+\epsilon^2} \simeq m_{\tilde{A}'}$, because the viable parameter range has $\epsilon \ll 1$. The dark matter particles are thereby coupled to the standard model fermions with a coupling constant ϵq , where ϵ is the kinetic mixing parameter. The first term in this interaction Lagrangian gives rise to the dark matter self-interactions.

Dark gauge bosons are produced in astrophysical environments such as supernova cores primarily via bremsstrahlung off of standard model particles. This bremsstrahlung occurs through the ϵq coupling to charged standard model particles, in this particular case the proton and pion. The rate of bremsstrahlung depends upon both ϵ and the mass of the A' . Consequently, supernova cooling can constrain the mixing ϵ as a function

of $m_{A'}$ for such models. Delineating such a constraint is the primary aim of this paper.

III. METHODS

We aim to estimate the rate of energy loss from the core of a supernova from A' bremsstrahlung during nucleon-nucleon interactions. The calculation is analogous to the well-known estimate of axion emission from supernova cores described in Ref. [51] and references therein, but is more complicated because the mass of the A' , unlike the mass of the axion, is not necessarily negligible. This section describes the calculation of the rate of energy loss from a supernova core from A' bremsstrahlung.

The bremsstrahlung process is not the only process with which we must be concerned. Clearly, the rate of bremsstrahlung will increase with ε ; however, ε can become sufficiently large that the radiated gauge bosons do not escape the supernova. This happens if the A' particles either decay to or interact with standard model particles prior to exiting the supernova core. In either case, the energy is not lost and the A' does not provide a cooling channel for the supernova. Consequently, for a given $m_{A'}$, there is a maximum ε that can be constrained in this manner. We estimate A' decay and scattering probabilities, and the upper limits on the ε constraints in this section as well. However, we note that terrestrial experiments generally rule out mixing parameters higher than the upper limits of the SN1987A forbidden region, so a precise estimate of these upper limits is not necessary.

A. Bremsstrahlung of A' Bosons

There are two processes to consider in order to estimate the rate of energy loss via A' bremsstrahlung. The first is proton-proton (pp) scattering with the bremsstrahlung of the dark photon off the proton; $p + p \rightarrow p + p + A'$. The second is proton-neutron (pn) scattering with bremsstrahlung off of either the proton or the charged pion; $p + n \rightarrow p + n + A'$. We estimate the rates for these processes using the one-pion exchange (OPE) approximation for nucleon interactions. In the pp case, there are eight tree-level diagrams, with the emission of the A' from each of the external legs. One of these diagrams is shown in Fig. 1; the remaining seven diagrams come from placing the radiated A' on each of the other three protons and then, for each of these, interchanging the outgoing momenta. For the pn case, there are five diagrams, four of which are analogous to the pp diagram shown in Fig. 1. The fifth diagram, shown in Fig. 2,

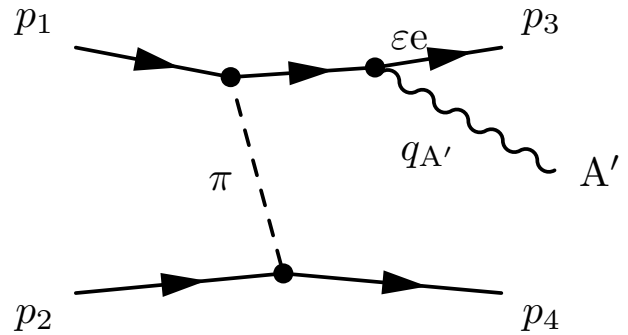


FIG. 1: One of the eight Feynman diagrams for the pp process. Three of the other diagrams are obtained by placing the A' on each of the protons in turn. The remaining four diagrams come from swapping the outgoing momenta.

corresponds to emission of the A' from the exchanged, charged pion.

Evaluating these diagrams is tedious, but very straightforward. The calculation differs from the well-known axion bremsstrahlung calculation exploited in a similar context [51], because the mass of the A' boson is not necessarily negligible in the kinematic region of interest for supernova explosions. The correct kinematical

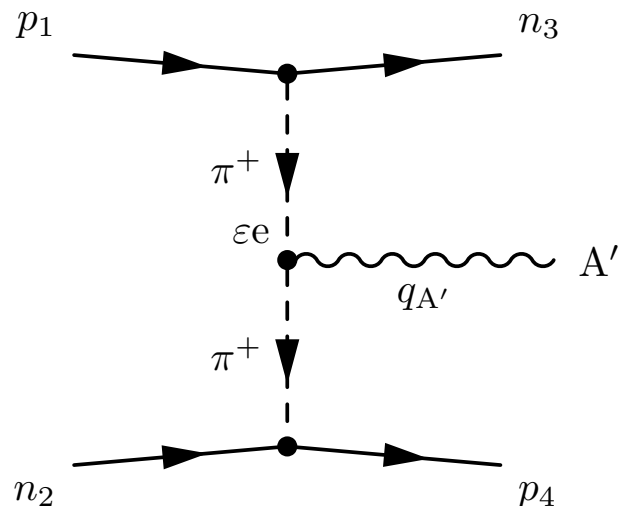


FIG. 2: One of the five Feynman diagrams for the pn process. This particular diagram shows internal bremsstrahlung off of the charged pion. The remaining four diagrams are analogous to the pp diagram shown in Fig. 1. In the case of the pn processes, there are only four diagrams for bremsstrahlung off of the external legs because two of the legs correspond to the uncharged neutron.

relations are

$$p_1 \cdot p_2 = M_N^2 - \frac{l^2}{2} - \frac{k^2}{2} + p_2 \cdot q_{A'}, \quad (2)$$

$$p_1 \cdot p_3 = M_N^2 + k \cdot l - \frac{k^2}{2} + p_3 \cdot q_{A'}, \quad (3)$$

$$p_1 \cdot p_4 = k \cdot l + M_N^2 - \frac{l^2}{2} + p_4 \cdot q_{A'}, \quad (4)$$

$$p_2 \cdot p_3 = M_N^2 - \frac{l^2}{2}, \quad (5)$$

$$p_2 \cdot p_4 = M_N^2 - \frac{k^2}{2}, \quad \text{and} \quad (6)$$

$$p_3 \cdot p_4 = k \cdot l + M_N^2 - \frac{l^2 + k^2}{2}, \quad (7)$$

where p_1 and p_2 are the four-momenta of the incoming nucleons, p_3 and p_4 are the momenta of the outgoing nucleons, $q_{A'}$ is the A' momentum, $k = p_2 - p_4$, $l = p_2 - p_3$, and M_N is the nucleon mass. These kinematical relations correct the relations in Ref. [52].

The eight diagrams contribute the following eight terms to the pp amplitude,

$$M_1 = \frac{4M_N^2}{m_\pi^2} \frac{f_{\text{pp}}^2 e \varepsilon}{k^2 - m_\pi^2} \frac{1}{m_{A'}^2 - 2q_{A'} \cdot p_1} \bar{u}(p_4) \gamma_5 u(p_2) \bar{u}(p_3) \gamma_5 (\not{p}_1 - q_{A'} + M_N) \not{\epsilon} u(p_1), \quad (8)$$

$$M_2 = -\frac{4M_N^2}{m_\pi^2} \frac{f_{\text{pp}}^2 e \varepsilon}{l^2 - m_\pi^2} \frac{1}{m_{A'}^2 - 2q_{A'} \cdot p_1} \bar{u}(p_3) \gamma_5 u(p_2) \bar{u}(p_4) \gamma_5 (\not{p}_1 - q_{A'} + M_N) \not{\epsilon} u(p_1), \quad (9)$$

$$M_3 = \frac{4M_N^2}{m_\pi^2} \frac{f_{\text{pp}}^2 e \varepsilon}{k^2 - m_\pi^2} \frac{1}{m_{A'}^2 - 2q_{A'} \cdot p_2} \bar{u}(p_3) \gamma_5 u(p_1) \bar{u}(p_4) \gamma_5 (\not{p}_2 - q_{A'} + M_N) \not{\epsilon} u(p_2), \quad (10)$$

$$M_4 = -\frac{4M_N^2}{m_\pi^2} \frac{f_{\text{pp}}^2 e \varepsilon}{l^2 - m_\pi^2} \frac{1}{m_{A'}^2 - 2q_{A'} \cdot p_2} \bar{u}(p_4) \gamma_5 u(p_1) \bar{u}(p_3) \gamma_5 (\not{p}_2 - q_{A'} + M_N) \not{\epsilon} u(p_2), \quad (11)$$

$$M_5 = \frac{4M_N^2}{m_\pi^2} \frac{f_{\text{pp}}^2 e \varepsilon}{k^2 - m_\pi^2} \frac{1}{m_{A'}^2 + 2q_{A'} \cdot p_3} \bar{u}(p_4) \gamma_5 u(p_2) \bar{u}(p_3) \not{\epsilon} (\not{p}_3 + q_{A'} + M_N) \gamma_5 u(p_1), \quad (12)$$

$$M_6 = -\frac{4M_N^2}{m_\pi^2} \frac{f_{\text{pp}}^2 e \varepsilon}{l^2 - m_\pi^2} \frac{1}{m_{A'}^2 + 2q_{A'} \cdot p_3} \bar{u}(p_4) \gamma_5 u(p_1) \bar{u}(p_3) \not{\epsilon} (\not{p}_3 + q_{A'} + M_N) \gamma_5 u(p_2), \quad (13)$$

$$M_7 = \frac{4M_N^2}{m_\pi^2} \frac{f_{\text{pp}}^2 e \varepsilon}{k^2 - m_\pi^2} \frac{1}{m_{A'}^2 + 2q_{A'} \cdot p_4} \bar{u}(p_3) \gamma_5 u(p_1) \bar{u}(p_4) \not{\epsilon} (\not{p}_4 + q_{A'} + M_N) \gamma_5 u(p_2), \quad (14)$$

$$M_8 = -\frac{4M_N^2}{m_\pi^2} \frac{f_{\text{pp}}^2 e \varepsilon}{l^2 - m_\pi^2} \frac{1}{m_{A'}^2 + 2q_{A'} \cdot p_4} \bar{u}(p_3) \gamma_5 u(p_2) \bar{u}(p_4) \not{\epsilon} (\not{p}_4 + q_{A'} + M_N) \gamma_5 u(p_1), \quad (15)$$

where the dark photon polarization is given by ϵ^ν . These expressions are identical to those given in Ref. [52]; however, they do not simplify significantly if the correct kinematics are used. Our squared matrix element contains over 200 terms, so we do not reproduce it here for reasons of convenience. However, we note that our result for $|\mathcal{M}_{\text{pp}}|^2$ is symmetric under exchange of k and l as

required.

The pn process contains four diagrams analogous to the diagrams for the pp process (only four, of course, because the neutrons cannot radiate the A'). The new diagram that is relevant in the pn process is shown in Fig. 2 and yields a contribution of

$$M'_5 = \frac{4M_N}{m_\pi} \frac{f_{\text{pn}}^2 e \varepsilon}{l^2 - m_\pi^2} \frac{1}{(l - q_{A'})^2 - m_\pi^2} \bar{u}(p_3) \gamma_5 u(p_1) \bar{u}(p_4) \gamma_5 u(p_2) (q_{A'} - 2l) \cdot \epsilon. \quad (16)$$

The pn processes likewise yields a squared amplitude,

$|\mathcal{M}_{\text{pn}}|^2$ that is unwieldy, so we do not give the the full

expression here. We provide mathematica notebooks detailing our computation of the amplitudes with this submission.

B. The Streaming Limit of the Energy Loss Rate

The first and simplest bound that may be obtained arises from assuming that all A' particles produced in the supernova core leave the supernova, carrying their energies with them. The constraint can be derived simply by requiring that the energy loss through this cooling channel be less than the cooling from neutrino emission; any greater, and it would have an observable effect on su-

pernova cooling. This calculation yields values of ε above which cooling through A' production is too rapid to be consistent with SN1987A. We will consider modifications to this bound from A' trapping and decay in subsequent subsections.

The quantity of interest is the rate of energy emission through dark gauge bosons. From the spin-summed, squared amplitudes described in the previous subsection, the energy emission rate is obtained by integrating over the phase space, and adding a factor of the energy of the emitted particle. To be specific, the energy emission rate per unit volume is

$$Q_i = (2\pi)^4 \int E_{A'} \sum_{s_1, s_2} |\mathcal{M}_i|^2 f(p_1) f(p_2) \delta^{(4)}(p_1 + p_2 - p_3 - p_4 - q_{A'}) d\Pi, \quad (17)$$

where

$$d\Pi = \frac{d^3\vec{q}_{A'}}{(2\pi)^3 2E_{A'}} \prod_{j=1}^4 \frac{d^3\vec{p}_j}{(2\pi^3) 2E_j} \quad (18)$$

is the Lorentz-invariant phase space interval, $E_{A'}$ is the energy of the emitted A' boson, $f(p)$ are the phase-space densities of the incoming nucleons, and the index i on Q_i refers to either the pp or pn processes. The nucleons in the core are comfortably non-degenerate and non-relativistic, so the Pauli blocking factor is omitted from Eq. (17) and we take all nucleons to have a Maxwell-Boltzmann phase-space distribution,

$$f(p) = \frac{n_b}{2} \left(\frac{2\pi}{M_N T} \right)^{3/2} \exp\left(-\frac{p^2}{2M_N T}\right). \quad (19)$$

We choose a baryon number density of $n_b \approx 1.8 \times 10^{38} \text{ cm}^{-3}$ and a core supernova temperature of $T = 30 \text{ MeV}$, both of which are typical choices and thought to be representative of supernova cores.

We performed the phase space integrals using the Monte Carlo routines in the CUBA library [60]. We integrated over the momenta $\vec{p}_1, \vec{p}_2, \vec{p}_3$, and the direction of the three-momentum of the radiated boson $\hat{q}_{A'}$, after fixing \vec{p}_4 and the magnitude of $\vec{q}_{A'}$ using the delta functions. We used the `suave` method provided within CUBA, which combines importance sampling and adaptive subdivision, as this method provided the best compromise between accuracy and run-time for this particular application.

To obtain the dark gauge boson luminosity from Q_{pp} and Q_{pn} , we assumed that A' production takes place in a stellar core of radius $\sim 1 \text{ km}$, so that the total luminosity of A' is

$$L_{A'} = V(Q_{pp} + Q_{pn}), \quad (20)$$

where V is the volume of the sphere, and the luminosity per unit mass within the core is

$$\left(\frac{L_{A'}}{M} \right) = \frac{Q_{pp} + Q_{pn}}{\rho}, \quad (21)$$

where $\rho = 3 \times 10^{14} \text{ g/cm}^3$ is the mass density of the core. Following previous studies, the energy loss rate into novel particles cannot exceed

$$\epsilon_{A'} = \left(\frac{L_{\max}}{M} \right) \approx 10^{19} \frac{\text{erg}}{\text{g} \cdot \text{s}} \quad (22)$$

without significantly reducing the duration of the neutrino burst observed at Earth for SN1987A [51]. Writing $\epsilon_{A'} = \varepsilon^2 I_{A'}(m_{A'}, T)$, we delineate the constraint on the dark photon mixing parameter by

$$\varepsilon \lesssim \sqrt{\frac{\epsilon_{A'}}{I_{A'}(m_{A'}, T)}}. \quad (23)$$

At this point, we note that Dent et al. in Ref. [52] took a value of $\epsilon_{A'}$ approximately three orders of magnitude larger than this generally accepted value. Remarkably, this nearly canceled the errors in their evaluation of Q_{pp} and Q_{pn} , so that they quote constraints that are within an order of magnitude of the correct result.

The constraint derived in this manner from Eq. (23) sets the lower limit on the exclusion band shown in Figure 3. We will discuss Fig. 3 in more detail below. If all of the A' produced in the core leave the supernova freely, all values of ε higher than those given by Eq. (23) would be ruled out. However, as we have already mentioned, ε can become sufficiently large that only a negligible amount of energy actually exits the supernova core. For large values of ε , this can occur because of either A' decays or A' scattering. These additional considerations place an upper limit on the values of ε for which this constraint applies, and we discuss these effects in the next two subsections.

C. The Decay Limit

One upper limit to the excluded values of ε may be found by considering decay of the dark bosons into Standard Model particles. Standard model particles will scatter and thermalize on a timescale much shorter than the timescale for the evolution of the core, so decays within the core contribute little to the supernova cooling.

The dark boson has a typical lifetime of

$$\tau_{A'} = \frac{3}{\varepsilon^2 \alpha m_{A'}}, \quad (24)$$

where α is the fine structure constant. Therefore, the typical travel distance to decay is given by

$$l = \beta \tau_{A'} = \frac{3q_{A'}}{\varepsilon^2 \alpha m_{A'}^2}, \quad (25)$$

and so the fraction escaping the supernova before decay may be estimated as (e.g., Ref. [58])

$$\exp\left(-\frac{r_{\text{decay}}}{l}\right) = \exp\left(-\frac{r_{\text{decay}} m_{A'}^2 \alpha \varepsilon^2}{3q_{A'}}\right), \quad (26)$$

where r_{decay} is chosen to be 10 km, since the density of the supernova drops quickly around that size. This approximation should be valid so long as the size of the supernova within which standard model decay products can interact and be thermalized is significantly larger than the region within which A' are produced, an assumption that should be satisfied comfortably. To account for the suppression of gauge boson luminosity due to decays we simply multiply the phase space integrand in Eq. (17) by the exponential suppression factor, after which the calculation proceeds as in the previous subsection. The limit is derived in the same way, with the additional complication that $I_{A'}$ is now a function of ε , in addition to $m_{A'}$ and T . The constraint Eq. (23), therefore, becomes a transcendental equation that must be solved numerically.

The luminosity in A' will be an increasing function of ε until decays suppress the gauge boson luminosity, at which point $L_{A'}$ becomes a rapidly decreasing function of ε . Therefore, the excluded values of ε at a given mass will generally have a lower bound set by the calculations of the previous subsection, and an upper bound set by decays. An approximate treatment of the upper bound due to decays, as we present here, is sufficient because over almost the entire mass range of interest, larger values of ε are independently excluded by terrestrial beam dump experiments [58]. Therefore, it is far more important to derive an accurate estimate of the *lower* boundary of the exclusion region (as was done in the previous subsection) than the upper boundary of the exclusion region.

D. Trapping limit

The second effect that produces an upper bound on the excluded region comes from considering trapping of dark bosons within the supernova. With a large enough coupling, the dark photons will thermalize and then will be emitted from an approximately spherical “dark photosphere” at the radial position where the A' mean free path becomes larger than the typical size of the supernova core. In this case the luminosity is given simply by Stefan’s law,

$$L_{A'} = 4\pi r_{\text{dp}}^2 T_{A'}^4 \sigma, \quad (27)$$

where r_{dp} is now the radius of the emitting shell and $T_{A'}$ its temperature. We estimate the radius of this dark photosphere as $r_{\text{dp}} = 10$ km, because the density of the supernova drops drastically around that point. We will confirm shortly that this estimate is consistent within the context of the simple model that we adopt for the interior structure of the supernova atmosphere. The bound on the luminosity can then be recast as a bound on $T_{A'}$,

$$T_{A'} \lesssim 9.6 \text{ MeV}. \quad (28)$$

That bound can then be translated into the desired bound on the coupling as a function of mass by adopting a simple model for the supernova atmosphere, assuming that the particles are emitted from the dark photosphere at a point where the optical depth to scattering is $\tau = 2/3$, and finding the temperature that corresponds to that optical depth.

This is a somewhat involved calculation. First, one needs a model for the density and temperature in the supernova. Following the simple, early model of Ref. [50], we assume a simple power-law model for the supernova

core, with

$$\rho = \rho_p \left(\frac{R}{r} \right)^n, \quad (29)$$

$$T = T_R \left[\frac{\rho(r)}{\rho_p} \right]^{1/3}, \quad (30)$$

with $\rho_p = 3 \times 10^{14} \text{ g/cm}^3$, $T_R = 30 \text{ MeV}$, $R = 10 \text{ km}$, and $n = 5$. The optical depth is given by

$$\tau = \int_{r_x}^{\infty} \kappa \rho \, dr, \quad (31)$$

where κ is the opacity, which we take to be the Rosseland mean

$$\frac{1}{\kappa \rho} = \frac{15}{4\pi^4 T^5} \int_{M_{A'}}^{\infty} \frac{E_{A'}^2 e^{E_{A'}/T} \sqrt{E_{A'}^2 - m_{A'}^2}}{(e^{E_{A'}/T} - 1)^2} l_{A'} \, dE_{A'}, \quad (32)$$

where $l_{A'}$ is the mean free path.

The inverse mean free path can be obtained by modifying Q_i , the expression for the energy loss rate, as follows: removing the factor of $E_{A'}$ and the phase space integral over $q_{A'}$, and adding a factor of $e^{E_{A'}/T}$ for detailed balance. This factor comes from turning the A' from an outgoing to an incoming state in the calculation (e.g., see Eq. (4.43) in Ref. [51]). This gives the inverse mean free path as a function of mass and coupling. Again, we perform the required integration numerically using the CUBA package. This then allows the calculation of κ_{pp} and κ_{pn} , which are the opacities due to inverse bremsstrahlung for proton-proton and proton-neutron processes respectively. These dominate the opacity of the star to A' propagation. The inverse opacities for the pn and pp processes add, giving the total opacity $\kappa^{-1} = \kappa_{pp}^{-1} + \kappa_{pn}^{-1}$.

Having obtained an expression for κ , we can now find the optical depth as follows. Define a typical optical depth as $\tau_R = \kappa_R \rho_R R$. We then have

$$\kappa \rho R = \tau_R \left(\frac{\rho}{\rho_R} \right)^2 \left(\frac{T_R}{T} \right)^{3/2}. \quad (33)$$

This can be combined with the previous expressions for the density and temperature as a function of position and plugged in to the integral expression for the optical depth to obtain

$$\tau = \int_{r_x}^{\infty} \tau_R \left(\frac{R}{r} \right)^{3n/2} \, dr \quad (34)$$

$$= \frac{\tau_R}{\frac{3n}{2} - 1} \left(\frac{T_{A'}}{T_R} \right)^{(9/2 - 3/n)}. \quad (35)$$

The bound on the coupling is obtained by requiring $\tau(\varepsilon, m_{A'}) \leq 2/3$. Note that strictly speaking we should

have determined r_{dp} rather than assuming a value. However, it is possible to verify the self-consistency of our assumption using this model for the supernova atmosphere. In particular, this model implies that an optical depth of $\tau = 2/3$ is reached at a radial position of $r_{dp} = 11 \text{ km}$, validating the assumption made at the outset. As we stated in the previous subsection, the approximate treatment of the upper limit of the exclusion region is justified by the fact that values of ε close to the upper limit of the exclusion region are ruled out by independent, terrestrial experiments.

IV. RESULTS

The considerations of the previous section lead to constraints on the viable parameters for dark electromagnetism models of SIDM, in particular, on the mixing parameter ε as a function of the dark photon mass $m_{A'}$. The excluded region is depicted in Fig. 3 as the shaded blue region. The lower limit of our excluded region lies at a value of ε about a factor of four larger than that of Dent et al. in Ref. [52] and is in excellent agreement with the result of Rrapaj and Reddy [53] despite the fact that they work with an SRA approximation and we work with a OPE model.

Figure 3 shows several other estimates of the lower bound on ε in an effort to elucidate possibly confusing points in the existing literature. As we stated earlier, the work of Ref. [52] contained several errors that partially cancelled each other. The black line in Fig. 3 represents our effort to reproduce the result of Ref. [52] using (incorrectly) the equations that they quote in their paper. However, Ref. [52] had significant errors in their calculations of the dark photon luminosity and chose an energy loss rate three orders of magnitude higher than other practitioners. Adopting the Dent et al. [52] equations for the dark photon luminosity, but the correct limit on the energy loss rate, results in the red line in Fig. 3. As Ref. [52], our primary result uses a OPE model for nucleon interactions, so the entirety of the difference between the red line and the lower bound of our exclusion region stems from an incorrect estimate of the bremsstrahlung rate in Ref. [52].

Rrapaj and Reddy [53] estimated A' luminosity using the SRA for nucleon interactions, which enabled them to use nuclear scattering data in the estimation of the bremsstrahlung rate. This approach overcomes the shortcomings of the OPE approximation, though at high dark photon masses this approximation breaks down. We have repeated the calculation in the SRA as described in Rrapaj and Reddy [53] and our result is shown as the purple

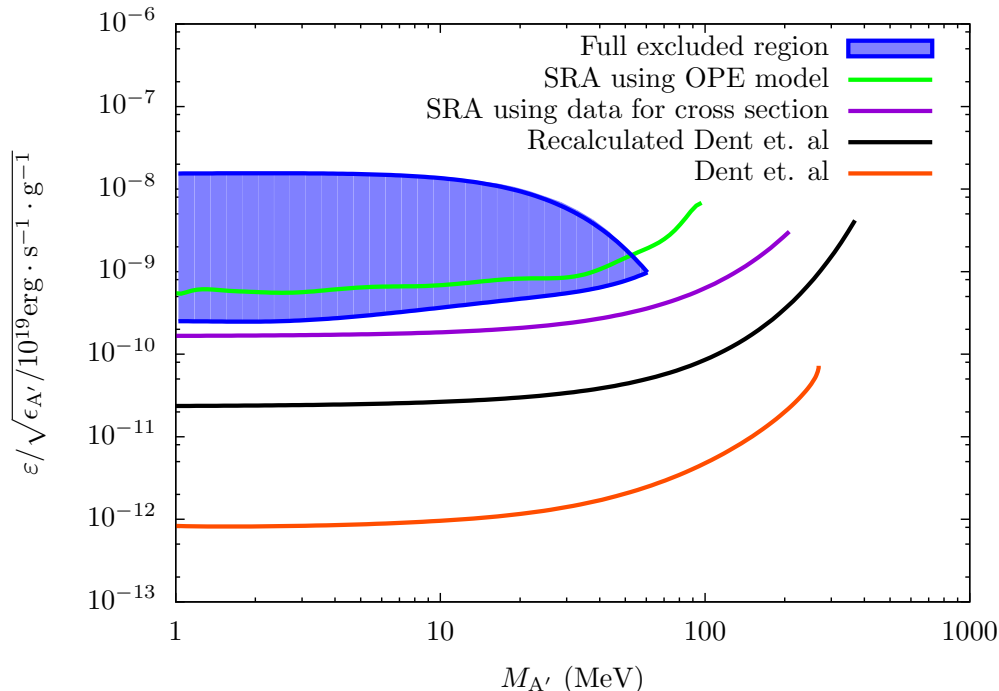


FIG. 3: Constraints on dark photon models. The constraint scales according to the assumed, maximal energy loss rate of $\epsilon_{A'} = 10^{19} \text{ erg g}^{-1} \text{ s}^{-1}$ as shown on the vertical axis label. Our primary result is the excluded region in the ϵ - $m_{A'}$ plane shaded in blue. The black curve is our attempt to reproduce exactly Ref. [52], while the red curve is Ref. [52] but with the correct luminosity constraint. The purple curve was computed by using the SRA and fixing the cross section through a polynomial fit to nuclear scattering data (e.g., see [53]), while the green curve uses the SRA of the OPE result.

line in Fig. 3. Our SRA result is in excellent agreement with Ref. [53]. It is also worth noting that the SRA and OPE approximations yield constraints on ϵ that agree quite well with each other. This suggests, of course, that the discrepancy between Ref. [52] and Ref. [53] stems primarily from errors in Ref. [52] and not to the OPE model of nucleon interactions. In an effort to estimate the possible shortcomings of the SRA approximation, the green line in Fig. 3 shows the lower bound on the excluded region that we drive using the SRA along with OPE expressions for nucleon scattering cross sections. As one can see, the SRA is in good agreement with the full OPE bound. Consequently, we suggest that use of the SRA in this context results in an overestimate of the lower limit on ϵ of less than a factor or three.

V. DISCUSSION

We have revisited constraints on SIDM models in which the self-interaction arises from dark electromagnetism. We have constrained the mixing parameter for models in which the dark photon mixes with the standard model photon through a kinetic mixing term. Our

calculation is similar to previous work in Ref. [52] and Ref. [53] and is aimed at clarifying some confusion in the literature on this subject that may stem from several errors in the calculation of Ref. [52].

Our constraints on the mixing parameter are shown in Fig. 3 and agree well with the those presented in Ref. [53] and, for dark photon masses $m_{A'} \gtrsim 10 \text{ MeV}$, Ref. [54]. We argue that the lower bound on the dark photon mixing parameter is only sensitive to the SRA to within a factor of ~ 3 or less. A more precise constraint on such models from SN1987A is probably not practicable because the interior temperature of the SN1987A core is somewhat uncertain and this uncertainty alone gives rise to an uncertainty in the excluded region of at least a factor of ~ 2 . Finally, Hardy and Lasenby [54] consider plasma effects within the supernova. The most important ramification of this work in the context of our paper is that it demonstrates that constraints on ϵ should be significantly weakened relative to our results in the mass range $m_{A'} \lesssim 10 \text{ MeV}$.

Finally, we note that the interior temperature and density within the progenitor of SN1987A remain uncertain at least at the level of several tens of percent [e.g.

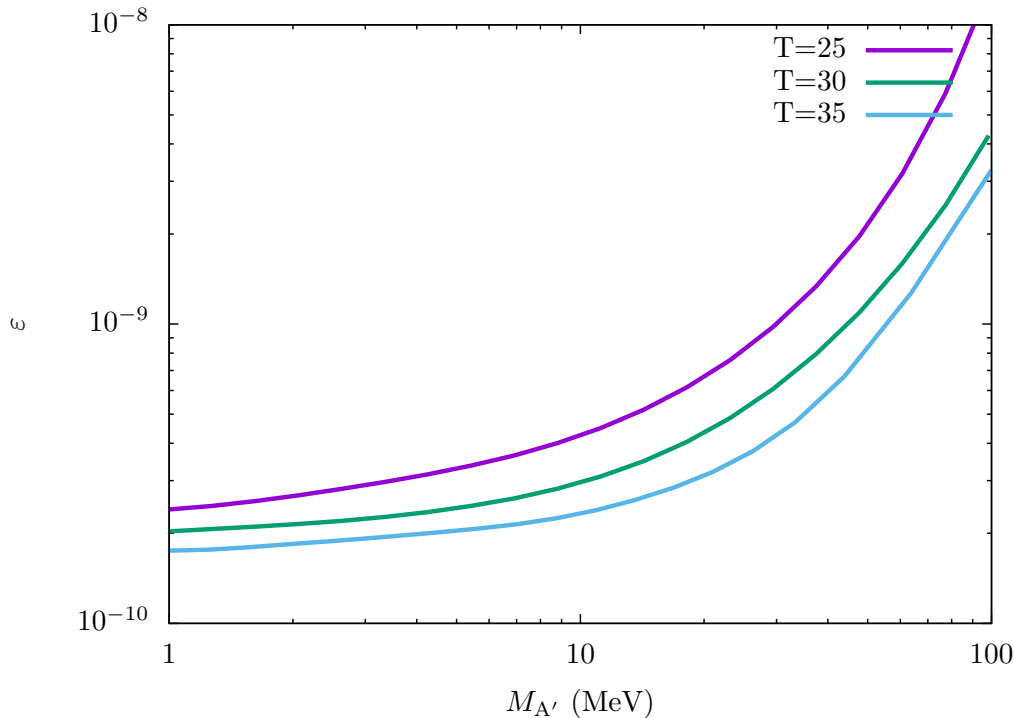


FIG. 4: Effect of changing the core temperature on the lower bound of the dark photon constraint. The calculation that produced the blue line of Fig. 3 was repeated for core temperatures of 25 MeV, 30 MeV, and 35 MeV. In this case the energy loss rate was throughout taken to be $\epsilon_{A'} = 10^{19} \text{ erg g}^{-1} \text{ s}^{-1}$

61, 62]. This is well worth noting because the constraints one derives using the techniques in this work or similar techniques are quite sensitive to the properties of the SN1987A core, particularly the core temperature. As an example of this, we have repeated a portion of our calculations after shifting the core temperature by ± 5 MeV. This result is shown in Figure 4. We find that the lower boundary of the excluded region shifts by a factor of ~ 2 at low mass ($m_{A'} \lesssim T$ where $T = 30$ MeV in our fiducial calculation, following work of previous authors) and considerably more at high mass. We conclude that the differences among theoretical techniques for computing the excluded region (OPE, SRA, ...) lead to uncertainties that are of the same order or smaller than the uncertainty in the excluded region induced by our limited knowledge of the properties of the SN1987A progenitor interior. The excluded regions we and other authors de-

lineate should be considered to be uncertain by a factor of ~ 3 . Refining the theoretical approach to this problem is therefore unwarranted until a breakthrough in our understanding of the interior of the SN1987A progenitor is achieved.

Acknowledgments

We thank Carles Badenes, John Hillier, and Francis Timmes for guidance in understanding the state of knowledge of the SN1987A progenitor. AKL was supported in part by NSF grant PHY-1519175. ARZ was supported in part by the DoE through Grant DE-SC0007914 and by the Pittsburgh Particle physics Astrophysics and Cosmology Center (Pitt PACC) at the University of Pittsburgh.

-
- [1] G. Jungman, M. Kamionkowski, and K. Griest, Phys. Reports **267**, 195 (1996).
 [2] E. D. Carlson, M. E. Machacek, and L. J. Hall, Astrophys. J. **398**, 43 (1992).
 [3] A. A. de Laix, R. J. Scherrer, and R. K. Schaefer, Astro-

- phys. J. **452**, 495 (1995), arXiv:astro-ph/9502087.
 [4] F. Atrio-Barandela and S. Davidson, Phys. Rev. D **55**, 5886 (1997), arXiv:astro-ph/9702236.
 [5] D. N. Spergel and P. J. Steinhardt, Phys. Rev. Lett. **84**, 3760 (2000), arXiv:astro-ph/9909386.

- [6] C. J. Hogan and J. J. Dalcanton, *Phys. Rev. D* **62**, 063511 (2000), arXiv:astro-ph/0002330.
- [7] R. N. Mohapatra and V. L. Teplitz, *Phys. Rev. D* **62**, 063506 (2000), arXiv:astro-ph/0001362.
- [8] R. Davé, D. N. Spergel, P. J. Steinhardt, and B. D. Wandelt, *Astrophys. J.* **547**, 574 (2001), arXiv:astro-ph/0006218.
- [9] J. Hisano, S. Matsumoto, and M. M. Nojiri, *Phys. Rev. Lett.* **92**, 031303 (2004), arXiv:hep-ph/0307216.
- [10] J. Hisano, S. Matsumoto, M. M. Nojiri, and O. Saito, *Phys. Rev. D* **71**, 063528 (2005), arXiv:hep-ph/0412403.
- [11] M. Pospelov, A. Ritz, and M. Voloshin, *Phys. Lett. B* **662**, 53 (2008), 0711.4866.
- [12] N. Arkani-Hamed, D. P. Finkbeiner, T. R. Slatyer, and N. Weiner, *ArXiv e-prints* (2008), 0810.0713.
- [13] M. Lattanzi and J. Silk, *ArXiv e-prints* (2008), 0812.0360.
- [14] L. Ackerman, M. R. Buckley, S. M. Carroll, and M. Kamionkowski, *Phys. Rev. D* **79**, 023519 (2009), 0810.5126.
- [15] J. L. Feng, M. Kaplinghat, H. Tu, and H.-B. Yu, *Journal of Cosmology and Astro-Particle Physics* **7**, 4 (2009), 0905.3039.
- [16] K. Kong, G. Mohlabeng, and J.-C. Park, *Physics Letters B* **743**, 256 (2015), 1411.6632.
- [17] M. R. Buckley and P. J. Fox, *Phys. Rev.* **D81**, 083522 (2010), 0911.3898.
- [18] K. K. Boddy, J. L. Feng, M. Kaplinghat, and T. M. P. Tait, *Phys. Rev.* **D89**, 115017 (2014), 1402.3629.
- [19] K. K. Boddy, J. L. Feng, M. Kaplinghat, Y. Shadmi, and T. M. P. Tait, *Phys. Rev.* **D90**, 095016 (2014), 1408.6532.
- [20] K. K. Boddy, M. Kaplinghat, A. Kwa, and A. H. G. Peter, *Phys. Rev.* **D94**, 123017 (2016), 1609.03592.
- [21] N. Yoshida, V. Springel, S. D. M. White, and G. Tormen, *Astrophys. J. Lett.* **544**, L87 (2000), arXiv:astro-ph/0006134.
- [22] O. Y. Gnedin and J. P. Ostriker, *Astrophys. J.* **561**, 61 (2001), arXiv:astro-ph/0010436.
- [23] J. Miralda-Escudé, *Astrophys. J.* **564**, 60 (2002).
- [24] S. W. Randall, M. Markevitch, D. Clowe, A. H. Gonzalez, and M. Bradač, *Astrophys. J.* **679**, 1173 (2008), 0704.0261.
- [25] M. Kamionkowski and S. Profumo, *Phys. Rev. Lett.* **101**, 261301 (2008).
- [26] A. R. Zentner, *Phys. Rev. D* **80**, 063501 (2009), 0907.3448.
- [27] B. E. Robertson and A. R. Zentner, *Phys. Rev. D* **79**, 083525 (2009), 0902.0362.
- [28] L. Pieri, M. Lattanzi, and J. Silk, *ArXiv e-prints* (2009), 0902.4330.
- [29] D. Spolyar, M. Buckley, K. Freese, D. Hooper, and H. Murayama, *ArXiv e-prints* (2009), 0905.4764.
- [30] D. P. Finkbeiner, T. Lin, and N. Weiner, *ArXiv e-prints* (2009), 0906.0002.
- [31] T. R. Slatyer, N. Padmanabhan, and D. P. Finkbeiner, *ArXiv e-prints* (2009), 0906.1197.
- [32] J. Bramante, K. Fukushima, J. Kumar, and E. Stopnitzky, *Phys. Rev. D* **89**, 015010 (2014), 1310.3509.
- [33] I. F. M. Albuquerque, C. Pérez de los Heros, and D. S. Robertson, *J. Cosmol. Astropart. Phys.* **2**, 047 (2014), 1312.0797.
- [34] M. Kaplinghat, S. Tulin, and H.-B. Yu, *Phys. Rev. D* **89**, 035009 (2014), 1310.7945.
- [35] C.-S. Chen, F.-F. Lee, G.-L. Lin, and Y.-H. Lin, *J. Cosmol. Astropart. Phys.* **10**, 049 (2014), 1408.5471.
- [36] J. L. Feng, J. Smolinsky, and P. Tanedo, *Phys. Rev. D* **93**, 115036 (2016).
- [37] R. Catena and A. Widmark, *J. Cosmol. Astropart. Phys.* **12**, 016 (2016), 1609.04825.
- [38] M. Markevitch, A. H. Gonzalez, D. Clowe, A. Vikhlinin, L. David, W. Forman, C. Jones, S. Murray, and W. Tucker, *Astrophys. J.* **606**, 819 (2004), astro-ph/0309303.
- [39] J. Zavala, M. Vogelsberger, and M. G. Walker, *Monthly Notices of the Royal Astronomical Society: Letters* **431**, L20 (2013), 1211.6426.
- [40] M. Rocha, A. H. G. Peter, J. S. Bullock, M. Kaplinghat, S. Garrison-Kimmel, J. Onorbe, and L. A. Moustakas, *Mon. Not. Roy. Astron. Soc.* **430**, 81 (2013), 1208.3025.
- [41] A. H. G. Peter, M. Rocha, J. S. Bullock, and M. Kaplinghat, *Mon. Not. Roy. Astron. Soc.* **430**, 105 (2013), 1208.3026.
- [42] F. Kahlhoefer, K. Schmidt-Hoberg, M. T. Frandsen, and S. Sarkar, *Mon. Not. Roy. Astron. Soc.* **437**, 2865 (2014), 1308.3419.
- [43] O. D. Elbert, J. S. Bullock, S. Garrison-Kimmel, M. Rocha, J. Oorbe, and A. H. G. Peter, *Mon. Not. Roy. Astron. Soc.* **453**, 29 (2015), 1412.1477.
- [44] J. L. Feng, J. Smolinsky, and P. Tanedo, *Phys. Rev.* **D93**, 015014 (2016), 1509.07525.
- [45] E. Del Nobile, M. Kaplinghat, and H.-B. Yu, *JCAP* **1510**, 055 (2015), 1507.04007.
- [46] J. L. Feng, J. Smolinsky, and P. Tanedo, *Phys. Rev.* **D93**, 115036 (2016), 1602.01465.
- [47] G. A. Dooley, A. H. G. Peter, M. Vogelsberger, J. Zavala, and A. Frebel, *Mon. Not. Roy. Astron. Soc.* **461**, 710 (2016), 1603.08919.
- [48] S. Y. Kim, A. H. G. Peter, and D. Wittman (2016), 1608.08630.
- [49] T. Bringmann, F. Kahlhoefer, K. Schmidt-Hoberg, and P. Walia, *Phys. Rev. Lett.* **118**, 141802 (2017), 1612.00845.
- [50] M. S. Turner, *Physical Review Letters* **60**, 1797 (1988).
- [51] G. G. Raffelt, *Stars as laboratories for fundamental physics : the astrophysics of neutrinos, axions, and other weakly interacting particles* (University of Chicago Press, 1996).
- [52] J. B. Dent, F. Ferrer, and L. M. Krauss, *ArXiv e-prints* (2012), 1201.2683.
- [53] E. Rrapaj and S. Reddy, *Phys. Rev. C* **94**, 045805 (2016), 1511.09136.
- [54] E. Hardy and R. Lasenby, *Journal of High Energy Physics* **2**, 33 (2017), 1611.05852.
- [55] D. Kazanas, R. N. Mohapatra, S. Nussinov, V. L. Teplitz, and Y. Zhang, *Nucl. Phys.* **B890**, 17 (2014), 1410.0221.
- [56] Y. Zhang, *JCAP* **1411**, 042 (2014), 1404.7172.
- [57] J. H. Chang, R. Essig, and S. D. McDermott, *JHEP* **01**, 107 (2017), 1611.03864.
- [58] J. D. Bjorken, R. Essig, P. Schuster, and N. Toro, *Phys. Rev. D* **80**, 075018 (2009), 0906.0580.
- [59] M. Kaplinghat, S. Tulin, and H.-B. Yu, *ArXiv e-prints* (2013), 1308.0618.
- [60] T. Hahn, *Comput. Phys. Commun.* **168**, 78 (2005), hep-ph/0404043.
- [61] A. Perego, M. Hempel, C. Fröhlich, K. Ebinger, M. Eichler, J. Casanova, M. Liebendörfer, and F.-K. Thielemann, *Astrophys. J.* **806**, 275 (2015), 1501.02845.
- [62] R. Farmer, C. E. Fields, I. Petermann, L. Dessart,

M. Cantiello, B. Paxton, and F. X. Timmes, *Astrophys. J. Supp. Ser.* **227**, 22 (2016), 1611.01207.